THE PROTEIN SOCIETY

FOR THE RECORD

K114 (*trans, trans*)-bromo-2,5-bis (4-hydroxystyryl)benzene is an efficient detector of cationic amyloid fibrils

Veli Selmani, Kevin J. Robbins, Valerie A. Ivancic, and Noel D. Lazo*

Carlson School of Chemistry and Biochemistry, Clark University, Worcester, Massachusetts, 01610

Received 20 September 2014; Revised 1 December 2014; Accepted 5 December 2014
DOI: 10.1002/pro.2620
Published online 18 December 2014 proteinscience.org

Abstract: Cationic amyloid fibrils found in human semen enhance the transmission of the human immunodeficiency virus (HIV) and thus, are named semen-derived enhancer of virus infection (SEVI). The mechanism for the enhancement of transmission is not completely understood but it has been proposed that SEVI neutralizes the repulsion that exists between the negatively charged viral envelope and host cell membrane. Consistent with this view, here we show that the fluorescence of cationic thioflavin T (ThT) in the presence of SEVI is weak, and thus ThT is not an efficient detector of SEVI. On the other hand, K114 ((*trans*, *trans*)-bromo-2,5-bis(4-hydroxystyryl)benzene) forms a highly fluorescent, phenolate-like species on the cationic surface of SEVI. This species does not form in the presence of amyloid fibrils from insulin and amyloid-β protein, both of which are efficiently detected by ThT fluorescence. Together, our results show that K114 is an efficient detector of SEVI.

Keywords: amyloid fibrils; SEVI; amyloid detection; ThT fluorescence; K114 fluorescence

Introduction

Many human diseases, including Alzheimer's disease, Parkinson's disease, and type 2 diabetes, are associated with amyloid fibrils.[1] A recent finding has further increased the association of amyloid fibrils with disease. Amyloid fibrils found in semen have been implicated in the enhanced transmission of the human immunodeficiency virus (HIV).[2–5] Among the amyloid fibrils found in semen, semen-derived enhancer of virus infection (SEVI) was the first to be discovered and has received the greatest attention. SEVI results from the self-assembly of a basic, 39-residue fragment of prostatic acid phosphatase (PAPf39) (Fig. 1).[2,3] SEVI is thought to enhance HIV infection by promoting the fusion of virions to cells by acting as a polycationic bridge that eliminates the electrostatic repulsion between the virions and target cells both of which possess negatively charged surfaces.[2,6,7] A mutated form of PAPf39 where all lysine and arginine residues were replaced with alanine forms amyloid fibrils that do not bind virions or promote infection.[6] Importantly, the

Abbreviations: HIV, human immunodeficiency virus; SEVI, semen-derived enhancer of virus infection; NOESY, nuclear Overhauser effect spectroscopy; PBS, phosphate-buffered saline; HFIP, 1,1,1,3,3,3-hexafluoroisopropanol; CD, circular dichroism; TEM, transmission electron microscopy; DMSO, dimethylsulfoxide; DSS, dimethyl-2-silapentane-5-sulphonate; MOE, Molecular Operating Environment.

Additional Supporting Information may be found in the online version of this article.

*Correspondence to: Noel D. Lazo, Carlson School of Chemistry and Biochemistry, Clark University, 950 Main Street, Worcester, MA 01610. E-mail: nlazo@clarku.edu

GIHKQKEKSRLQGGVLVNEILNHMKRATQIPSYKKLIMY

Figure 1. Primary structure of residues 248–286 of prostatic acidic phosphatase (PAPf39). The polypeptide is basic with a pI of 10.21. Residues that are predominantly charged at physiological pH include lysine and arginine (in red) which are positively charged and glutamate (in green) which is negatively charged. Residues found in the N-terminus of the polypeptide (underlined) do not form part of the core of SEVI.

magnitude of enhancement of HIV infection by semen samples correlates with the levels of SEVI.[8,9]

SEVI is thus, an important target for the development of strategies that will prevent the spread of HIV. One attractive strategy is to inhibit SEVI formation or disassemble pre-formed SEVI using small molecules. An efficient detector of SEVI thus will be useful in reporting the efficacy of anti-SEVI agents. Here, we show that thioflavin T (ThT), the most widely used molecule for the detection of amyloid fibrils in solution,[10–12] is not an efficient detector of SEVI. On the other hand, an analogue of Congo red, K114 [(*trans*, *trans*)-bromo-2,5-bis(4-hydroxystyryl)-benzene],[13] efficiently detects SEVI at physiologically-relevant concentrations through the formation of a phenolate-like species that is facilitated by the positively charged surface of SEVI.

Results and Discussion

The small molecule that is most widely used to detect amyloid fibrils in solution is thioflavin T (ThT).[10–12] It contains a dimethylaminobenzene ring and a cationic benzothiazole ring [Fig. 2(A)]. The basis for detection is simple: the binding of the molecule on the fibril surface leads to a dramatic enhancement in ThT fluorescence.[10,11,14–18] Because the amyloid fibrils from PAPf39 are cationic, we hypothesized that the binding of ThT is suboptimal and thus the enhancement of ThT fluorescence will be weak. Figure 2(B) presents fluorescence spectra of ThT in the presence of amyloid fibrils from PAPf39 and insulin. Both spectra show maximum fluorescence intensities at 483 nm. However, the enhancement of ThT fluorescence at 483 nm in the presence of SEVI is only 8× relative to the emission intensity of ThT in buffer at 483 nm, much less than the enhancement observed (213×) in the presence of a similar amount of amyloid fibrils from insulin.

Recently, we showed that the dramatic enhancement of ThT fluorescence in the presence of amyloid fibrils from insulin correlates with the NMR-detected on–off binding of ThT on the fibril surface.[18] The on–off binding was revealed by exchange-transferred nuclear Overhauser effect spectroscopy (NOESY),[19] by which exchange-transferred NOE cross peaks due to cross relaxation between protons in ThT were observed.[18] These cross peaks were not detected in ThT in buffer only. Together, our data indicate that the cross relaxation between protons in ThT was developed in its bound state and that the exchange between bound and free ThT is fast within the NMR timescale such that the NOE's in the bound state are transferred to the resonances of free ThT. We acquired NOESY spectra of ThT in the presence of SEVI. No exchange-transferred NOE cross peaks were observed (Supporting Information Fig. S1), indicating that the NMR-detected on–off binding of ThT on the fibril surface does not exist.

The absence of NMR-detected on–off binding of ThT on the surface of SEVI may be explained by electrostatic effects. Studies of SEVI using hydrogen-deuterium exchange mass spectrometry and protease protection assay have indicated that the N-terminus of PAPf39 (residues 1–9) (Fig. 1) is excluded from the fibril core and thus accessible to exchange and proteolytic attack.[20] This region contains three positively charged lysine residues (Fig. 1) that will interact unfavorably with the cationic

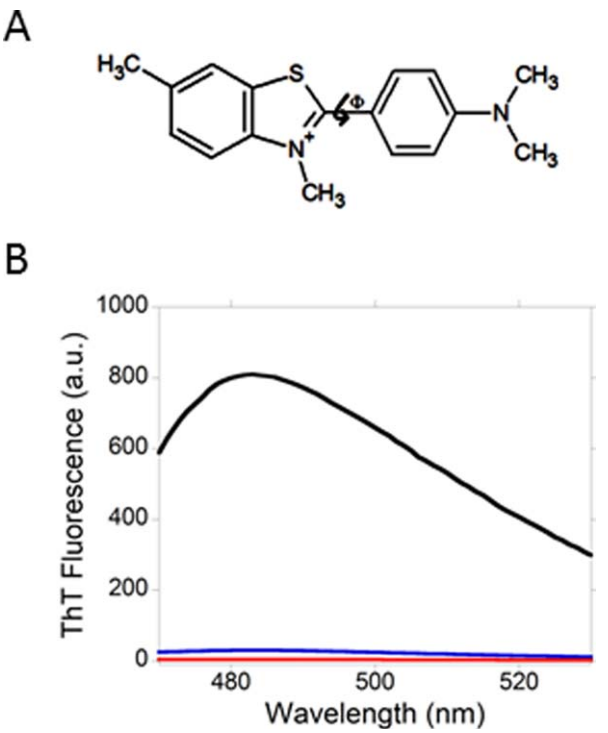

Figure 2. Thioflavin T (ThT) and its fluorescence in the presence of SEVI and amyloid fibrils from insulin. (A) ThT is a cationic molecule that contains a positively charged benzothiazole ring and a dimethylaminobenzene ring. The twisting of the two rings relative to one another defines the torsion angle ϕ. (B) The enhancement of ThT fluorescence in the presence of SEVI is much less than the enhancement of ThT fluorescence in the presence of amyloid fibrils from insulin. Emission spectra of ThT in buffer (red), ThT in the presence of SEVI (blue) and ThT in the presence of amyloid fibrils from insulin (black) are shown. The concentration of ThT in the three samples is 100 μM. The ThT:insulin and ThT:PAPf29 ratios in the fibril-containing samples were fixed at 1:1 (mole:mole).

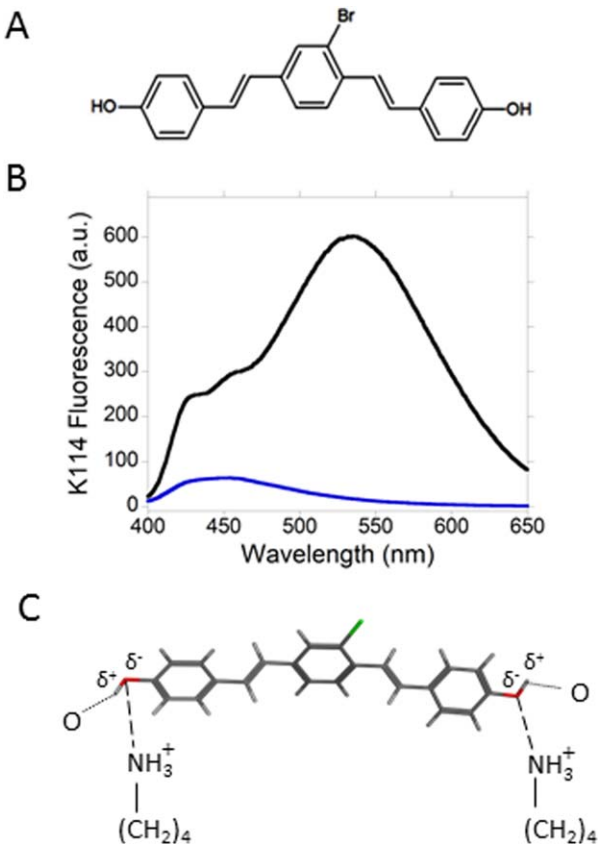

Figure 3. K114 *(trans,trans)*-1-bromo-2,5-bis(4-hydroxystyryl)benzene) and its fluorescence in the presence of SEVI. (A) K114 is a neutral molecule that contains two phenol groups which ionize to form phenolate species at basic pH. (B) The fluorescence of K114 is dramatically enhanced and shifted to longer wavelengths in the presence of SEVI. Emission spectra of K114 in the presence of unfibrillized PAPf39 (blue) and in the presence of SEVI (black). The position of maximum emission in the presence of SEVI is notably red-shifted to 535 nm. At this wavelength, the fluorescence intensity in the presence of SEVI is 35× higher than that in the presence of unfibrillized PAPf39. The concentration of K114 is 10 μ*M* and the K114:PAPf39 ratio is 1:2 (mole:mole) in both samples. (C) Schematic representation of the binding mode of K114 on the surface of SEVI. K114 forms a phenolate-like species that interacts with lysine residues found on the fibril surface.

ThT molecule. ThT has been shown by others to have low affinity for other amyloid fibrils with cationic surfaces including fibrils from the fibril-forming domain of the HET-s fungal prion protein[21] and from the model peptide KLKLKLELELELG.[22,23]

Because the surface of the amyloid fibrils from PAPf39 is cationic, we hypothesized that a small molecule that has the ability to form a negatively charged fluorescent species would be an efficient detector of the fibrils. The dye K114, (*trans,trans*)-1-bromo-2,5-bis(4-hydroxystyryl)benzene [Fig. 3(A)], forms a highly fluorescent phenolate anion at highly basic pH (pH > 9.5), whose maximum emission is significantly red-shifted to 520 nm, relative to that of unionized K114.[13] Because K114 is highly insoluble in aqueous solvents, we prepared stock solutions of the dye in dimethylsulfoxide (DMSO). An aliquot of the stock solution was then added to freshly dissolved PAPf39 phosphate-buffered saline (PBS) (pH 7.4) and to dispersions of SEVI in the same buffer. The amount of DMSO in these samples was kept at 1% (v/v). Electron microscopy of SEVI in the presence of K114 (Supporting Information Fig. S2) did not show the presence of dye aggregates that could lead to quenching of K114 fluorescence.[13] Figure 3(B) presents fluorescence spectra of K114 in the presence of freshly dissolved PAPf39 and in the presence of SEVI. The fluorescence spectrum of K114 in the presence of SEVI was dramatically enhanced and the location of maximum emission intensity is notably red-shifted to 535 nm. We attribute the red-shift to the formation of a phenolate-like species from K114. Figure 3(C) shows a schematic representation of how a phenolate-like species from energy-minimized K114 may be formed on the surface of SEVI. The partially negative oxygen atoms of the hydroxyl groups of K114 form attractive electrostatic interactions with the positively charged lysine residues. Additional stabilization may occur from hydrogen bonding between the hydroxyl protons of K114 and electronegative atoms on the fibril surface. There is precedence in the literature for lysine-phenolate electrostatic interactions. Studies of structure–function correlations in fructose-1,6-bisphosphate muscle aldolase, an essential glycolytic enzyme, indicate that a lysine residue stabilizes a phenolate ion formed as a result of proton transfer from a tyrosine residue.[24]

K114 fluorescence spectra in the presence of amyloid fibrils from amyloid-β 1-42 (Aβ42) (pH 4.3) and insulin (pH 2) were recorded to compare them with the K114 fluorescence data collected in the presence of SEVI (pH 7.4). K114 fluorescence is significantly enhanced in the presence of insulin or Aβ42 fibrils [Fig. 4(A)]. However, the emission spectra are not red-shifted relative to the emission spectrum of K114 in pure buffer. To better visualize the differences in the shifts in the emission spectra of K114 in the presence of amyloid fibrils from the three precursors studied here, the fluorescence spectra of K114 in the presence of amyloid fibrils from PAPf39, Aβ42 and insulin were plotted together as shown in Figure 4(B). The location of maximum emission of K114 in the presence of SEVI is dramatically red-shifted by 80 nm. Increasing the pH of the dispersion of amyloid fibrils from Aβ42 and insulin to 7.4 did not produce red-shifts in the emission spectra of K114 (Supporting Information Figs. S3 and S4). Together, our data suggest that the phenolate-like species from K114 which forms on the surface of SEVI does not form on the surface of amyloid fibrils from insulin and Aβ42. This result indicates that the surface of fibrils from insulin and Aβ42 are not cationic.

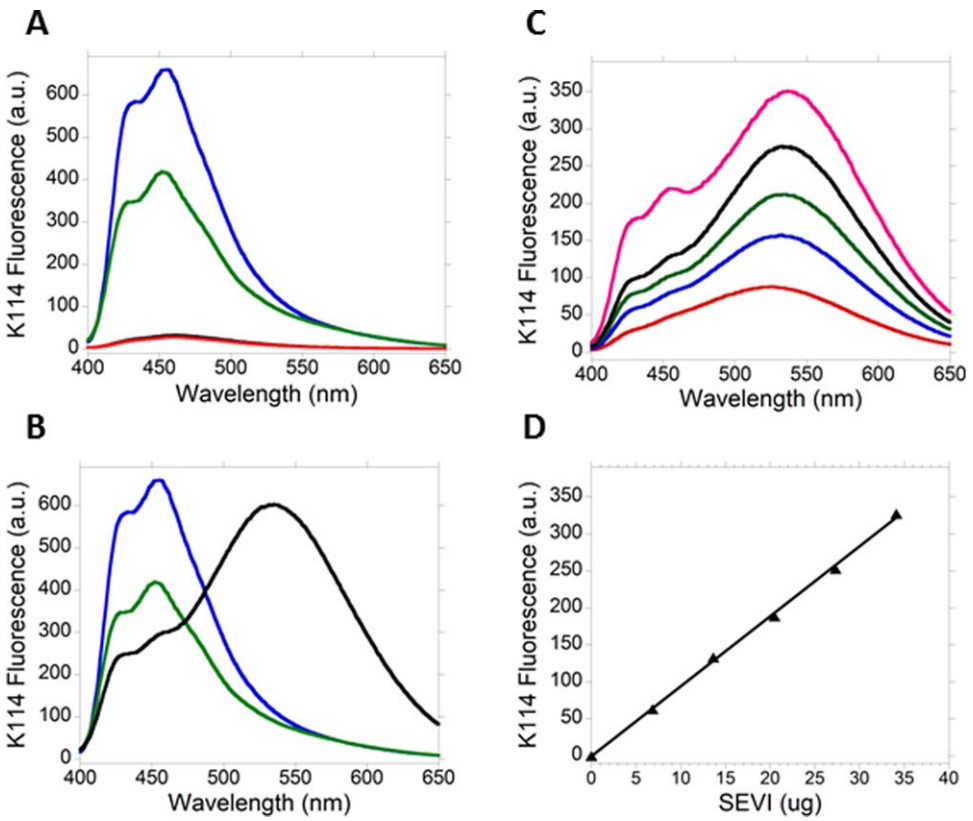

Figure 4. K114 fluorescence in the presence of amyloid fibrils from Aβ42, insulin and PAPf39. (A) The fluorescence of K114 is also dramatically enhanced in the presence of amyloid fibrils from insulin and Aβ42 but it is not shifted to longer wavelengths. Emission spectra of K114 in buffer only at pH 4.3 (red) and at pH 2 (black, overlaps with spectrum obtained at pH 4.3) and in the presence of amyloid fibrils from Aβ42 (green) and insulin (blue) are shown. The position of maximum emission in the spectra of samples that contain amyloid fibrils is at 455 nm. The concentration of K114 is 10 μ*M* in the four samples and the K114:protein ratio is 1:2 (mole:mole) in the samples with amyloid fibrils. (B) Emission spectra of K114 in the presence of amyloid fibrils from Aβ42 (green), insulin (blue) and PAPf39 (black). The position of maximum fluorescence of K114 in the presence of SEVI is dramatically red-shifted by 80 nm. (C) The fluorescence of K114 at 535 nm can be used to determine the amount of SEVI in solution. Emission spectra of K114 in the presence of 6.8 (red), 13.7 (blue), 20.5 (green), 27.3 (black), and 34.1 (magenta) μg of SEVI are shown. (D) The fluorescence intensity of K114 at 535 nm increases linearly with the amount of SEVI. The line is the result of linear regression as follows: $y = 9.46x$, $R = 0.99$. Each data point is the average of three separate measurements. The amount of SEVI in each sample was calculated by multiplying the molarity of the PAPf39 solution used in preparing fibrils by the molar mass of PAPf39 and the volume of the sample for K114 fluorescence (150 μL).

Münch and coworkers showed that SEVI-spiked semen enhanced HIV infection in a dose-dependent manner and that the required concentration of SEVI for enhancement to occur is in the μg/mL range.[2] Kim and coworkers later showed that semen-mediated HIV infection is donor dependent and correlates with the levels of SEVI in semen.[9] These results suggest that methods to rapidly detect and quantitate small amounts of SEVI in semen are needed. Figure 4(C) shows that the emission intensity of K114 increases with increasing amounts of SEVI in the sample. When fluorescence intensity at 535 nm was plotted against amounts of SEVI, a linear plot was obtained [Fig. 4(D)] suggesting that the emission intensity of K114 at 535 nm can be used to rapidly detect and quantitate amounts of SEVI in the μg range.

In summary, this work shows that ThT is not an efficient detector of SEVI because of suboptimal binding on the fibril surface due to unfavorable electrostatic interactions between the positively charged ThT molecule and the positively charged residues on the surface of SEVI. On the other hand, K114 detects SEVI with high efficiency due to its ability to form a fluorescent phenolate-like species on the positively charged surface of SEVI.

Materials and Methods

Preparation of fibrils

Human insulin was purchased from Sigma-Aldrich (St. Louis, MO). Peptides PAPf39 and Aβ42 were synthesized by NeoBioScience (Woburn, MA) and 21st Century Biochemicals (Marlborough, MA), respectively. Both were at least 95% pure as indicated by analytical reverse phase HPLC. Mass spectra of the peptides showed molecular masses consistent with theoretical values.

Insulin fibrils were prepared by dissolving insulin at a concentration of ~ 100 μ*M* in 10 mM sodium phosphate buffer (pH 2) with 10 mM NaCl.[18] The concentration of insulin was determined by UV absorbance at 275 nm using an extinction coefficient of 6,190 M^{-1} cm^{-1}.[25] The solution was then incubated at 70°C and monitored by circular dichroism (CD) until the α-helix to β-sheet transition was complete.

PAPf39 was dissolved at a concentration of ~300 μ*M* in pH 7.4 PBS buffer (8 m*M* NaH_2PO_4, 1.8 m*M* KH_2PO_4, 140 m*M* NaCl, 2.7 m*M* KCl). Peptide concentrations were determined by UV absorbance at 275 nm using an extinction coefficient of 2,980 M^{-1} cm^{-1}.[26] SEVI was prepared by incubating the solutions at 37°C with agitation at 1400 rpm in an Eppendorf thermomixer. Solutions were incubated until the random coil to β-sheet transition was complete as indicated by CD.

To disaggregate pre-formed assemblies, Aβ42 was pretreated with 1,1,1,3,3,3-hexafluoroisopropanol (HFIP). Briefly, the peptide was dissolved in 100% HFIP. After several minutes, the solution was then allowed to dry in a fume hood, and then lyophilized for 5 hr to completely remove the solvent. The lyophilized peptide was then dissolved in 10 m*M* sodium phosphate buffer (pH 7.4) and incubated at 37 °C in an Eppendorf thermomixer with mixing at 1000 rpm until the random coil to β-sheet transition was complete as monitored by CD.

Circular dichroism

Circular dichroic spectra were acquired at 25°C using a JASCO J-815 spectropolarimeter. Quartz cuvettes with a path length of 1 mm were used. Spectra were acquired from 260 to 195 nm at intervals of 1 nm using an averaging time of 4 s. For each sample, four spectra were acquired and then averaged.

Transmission electron microscopy (TEM)

Transmission electron microscopy was used to test for the presence of fibrils. An aliquot of the CD samples was placed on a carbon-coated copper grid and incubated for one minute. Excess solution was wicked off using tissue paper (Kimwipes). The sample was then stained with 1% aqueous uranyl acetate solution, dried with Kimwipe, incubated at room temperature for an additional 15–20 min to fully dry and then stored in the grid box holder until use. Micrographs were taken at the Core Electron Microscopy Facility of the University of Massachusetts Medical School.

Fluorescence spectroscopy

Ultra-pure ThT was purchased from AnaSpec Inc. (Fremont, CA). All samples for ThT fluorescence were prepared as follows. A concentrated stock solution of ThT was prepared in the same buffer used to prepare the amyloid fibril of interest. The concentration of ThT was determined by absorbance at 412 nm using an extinction coefficient of 32,000 M^{-1} cm^{-1}.[27] An aliquot of this solution was added to the peptide or protein sample of interest such that the ThT:peptide or protein ratio is 1:1 (mole:mole).

K114 was purchased from Sigma-Aldrich (St. Louis, MO). Samples for K114 fluorescence were prepared as follows. A stock solution of K114 (10 or 20 m*M*) was prepared in DMSO. An aliquot of the stock solution was added to the peptide or protein sample of interest such that the K114:peptide or protein ratio is 1:2. The concentration of DMSO in all samples was kept at 1% (v/v).

Fluorescence spectra were recorded using an Agilent Cary Eclipse spectrometer. Spectra of samples containing ThT were recorded from 450 to 600 nm following excitation at 440 nm. Spectra of samples containing K114 were recorded from 400 to 650 nm following excitation at 360 nm. Excitation and emission slit widths were set at 10 nm.

NMR spectroscopy

All samples for NMR were prepared in 99.9% D_2O, including: (i) ThT in buffer; (ii) ThT in the presence of amyloid fibrils from insulin; and (iii) ThT in the presence of SEVI. The concentration of ThT in all samples is 100 μ*M*. The ThT:protein or polypeptide ratio in samples (ii) and (iii) is 1:1 (mole:mole). All samples contained 2,2-dimethyl-2-silapentane-5-sulphonate (DSS) for chemical shift reference. A Varian INOVA spectrometer operating at 600 MHz and equipped with a 5 mm pulsed-field gradient triple resonance probe was used to acquire both one- and two-dimensional ^1H NMR spectra at 5°C. NOESY spectra were recorded using 384 t1 increments and 2K data points in t_2. Sixteen scans were acquired per t_1 increment. A relaxation delay of 2 s and mixing times of 10–400 ms were used.

Molecular modeling

A molecular model of K114 was built using the molecular builder tool in version 2012.10 of Molecular Operating Environment (MOE) (Chemical Computing Group, Montreal, Quebec, Canada). The potential energy of the molecule was minimized using the energy-minimization protocol in MOE and the MMFF94X force field that is parameterized for small molecules.

Acknowledgments

The authors thank Dr. Guoxing Lin for the maintenance of the NMR spectrometer used in this work.

References

1. Chiti F, Dobson CM (2006) Protein misfolding, functional amyloid, and human disease. Annu Rev Biochem 75:333–366.

2. Munch J, Rucker E, Standker L, Adermann K, Goffinet C, Schindler M, Wildum S, Chinnadurai R, Rajan D, Specht A, Gimenez-Gallego G, Sanchez PC, Fowler DM, Koulov A, Kelly JW, Mothes W, Grivel JC, Margolis L, Keppler OT, Forssmann WG, Kirchhoff F (2007) Semen-derived amyloid fibrils drastically enhance HIV infection. Cell 131:1059–1071.
3. Arnold F, Schnell J, Zirafi O, Sturzel C, Meier C, Weil T, Standker L, Forssmann WG, Roan NR, Greene WC, Kirchhoff F, Munch J (2012) Naturally occurring fragments from two distinct regions of the prostatic acid phosphatase form amyloidogenic enhancers of HIV infection. J Virol 86:1244–1249.
4. Olsen JS, DiMaio JT, Doran TM, Brown C, Nilsson BL, Dewhurst S (2012) Seminal plasma accelerates semen-derived enhancer of viral infection (SEVI) fibril formation by the prostatic acid phosphatase (PAP248–286) peptide. J Biol Chem 287:11842–11849.
5. Usmani SM, Zirafi O, Muller JA, Sandi-Monroy NL, Yadav JK, Meier C, Weil T, Roan NR, Greene WC, Walther P, Nilsson KP, Hammarstrom P, Wetzel R, Pilcher CD, Gagsteiger F, Fandrich M, Kirchhoff F, Munch J (2014) Direct visualization of HIV-enhancing endogenous amyloid fibrils in human semen. Nat Commun 5:3508.
6. Roan NR, Munch J, Arhel N, Mothes W, Neidleman J, Kobayashi A, Smith-McCune K, Kirchhoff F, Greene WC (2009) The cationic properties of SEVI underlie its ability to enhance human immunodeficiency virus infection. J Virol 83:73–80.
7. Castellano LM, Shorter J (2012) The surprising role of amyloid fibrils in HIV infection. Biology (Basel) 1:58–80.
8. Roan NR, Muller JA, Liu H, Chu S, Arnold F, Sturzel CM, Walther P, Dong M, Witkowska HE, Kirchhoff F, Munch J, Greene WC (2011) Peptides released by physiological cleavage of semen coagulum proteins form amyloids that enhance HIV infection. Cell Host Microbe 10:541–550.
9. Kim KA, Yolamanova M, Zirafi O, Roan NR, Staendker L, Forssmann WG, Burgener A, Dejucq-Rainsford N, Hahn BH, Shaw GM, Greene WC, Kirchhoff F, Munch J (2010) Semen-mediated enhancement of HIV infection is donor-dependent and correlates with the levels of SEVI. Retrovirology 7:55.
10. Groenning M (2010) Binding mode of Thioflavin T and other molecular probes in the context of amyloid fibrils-current status. J Chem Biol 3:1–18.
11. Amdursky N, Erez Y, Huppert D (2012) Molecular rotors: what lies behind the high sensitivity of the thioflavin-T fluorescent marker. Acc Chem Res 45: 1548–1557.
12. Biancalana M, Koide S (2010) Molecular mechanism of Thioflavin-T binding to amyloid fibrils. Biochim Biophys Acta 1804:1405–1412.
13. LeVine H, 3rd (2005) Mechanism of Aβ(1-40) fibril-induced fluorescence of (trans,trans)-1-bromo-2,5-bis(4-hydroxystyryl)benzene (K114). Biochemistry (Mosc) 44:15937–15943.
14. LeVine III H (1993) Thioflavine T interaction with synthetic Alzheimer's disease β-amyloid peptides: detection of amyloid aggregation in solution. Prot Sci 2:404–410.
15. Sulatskaya AI, Maskevich AA, Kuznetsova IM, Uversky VN, Turoverov KK (2010) Fluorescence quantum yield of thioflavin T in rigid isotropic solution and incorporated into the amyloid fibrils. PLoS One 5: e15385.
16. Sulatskaya AI, Kuznetsova IM, Turoverov KK (2012) Interaction of thioflavin T with amyloid fibrils: fluorescence quantum yield of bound dye. J Phys Chem B 116:2538–2544.
17. Robbins KJ, Liu G, Lin G, Lazo ND (2011) Detection of strongly bound Thioflavin T species in amyloid fibrils by ligand-detected ^{1}H NMR. J Phys Chem Lett 2:735–740.
18. Robbins KJ, Liu G, Selmani V, Lazo ND (2012) Conformational analysis of thioflavin T bound to the surface of amyloid fibrils. Langmuir 28:16490–16495.
19. Post CB (2003) Exchange-transferred NOE spectroscopy and bound ligand structure determination. Curr Opin Struct Biol 13:581–588.
20. French KC, Makhatadze GI (2012) Core sequence of PAPf39 amyloid fibrils and mechanism of pH-dependent fibril formation: the role of monomer conformation. Biochemistry (Mosc) 51:10127–10136.
21. Sabate R, Lascu I, Saupe SJ (2008) On the binding of Thioflavin-T to HET-s amyloid fibrils assembled at pH 2. J Struct Biol 162:387–396.
22. Khurana R, Coleman C, Ionescu-Zanetti C, Carter SA, Krishna V, Grover RK, Roy R, Singh S (2005) Mechanism of thioflavin T binding to amyloid fibrils. J Struct Biol 151:229–238.
23. Lazo ND, Downing DT (1997) β-helical fibrils from a model peptide. Biochem Biophys Res Commun 235: 675–679.
24. St-Jean M, Blonski C, Sygusch J (2009) Charge stabilization and entropy reduction of central lysine residues in fructose-bisphosphate aldolase. Biochemistry (Mosc) 48:4528–4537.
25. Sorci M, Grassucci RA, Hahn I, Frank J, Belfort G (2009) Time-dependent insulin oligomer reaction pathway prior to fibril formation: cooling and seeding. Proteins 77:62–73.
26. Shanmuganathan A, Bishop AC, French KC, McCallum SA, Makhatadze GI (2013) Bacterial expression and purification of the amyloidogenic peptide PAPf39 for multidimensional NMR spectroscopy. Prot Exp Purif 88:196–200.
27. Sulatskaya AI, Kuznetsova IM, Turoverov KK (2011) Interaction of thioflavin T with amyloid fibrils: stoichiometry and affinity of dye binding, absorption spectra of bound dye. J Phys Chem B 115:11519–11524.